Optical Stark Effect in the Two-Photon Spectrum of NO

Winifred M. Huo[a]
Radiation Laboratory, University of Notre Dame, Notre Dame, Indiana 46556

and

Kenneth P. Gross[a],[b]
Stanford University, Stanford, California 94305

and

Robert L. McKenzie
NASA Ames Research Center, Moffett Field, California 94035
(Received 18 June 1984)

A large optical Stark effect has been observed in the two-photon spectrum $X\,^2\Pi \rightarrow A\,^2\Sigma^+$ in nitric oxide. It is explained as a near-resonant process in which the upper state of the two-photon transition is perturbed by interactions with higher-lying electronic states coupled by the laser field. A theoretical analysis is presented along with Stark parameters determined from *ab initio* wave functions. The synthetic spectrum reproduces the major experimental features.

PACS numbers: 33.55.Be, 33.10.−n, 33.70.Jg, 33.80.Wz

In this Letter, we are reporting a quantitative determination of the optical Stark effect in a molecular, two-photon, electronic transition. In the past, optical Stark effects observed in resonant multiphoton transitions have been almost exclusively limited to atomic systems. As a result of the high density of states, molecular Stark effects are expected to be more easily observed, especially in multiphoton transitions using high laser intensities. In fact, such observations have been reported recently.[1-3] However, previous analyses of Stark effects in molecular multiphoton transitions have been limited to order-of-magnitude estimates.

During the course of developing a laser-induced fluorescence technique for gas-flow diagnostics, two of us[4,5] have studied two-photon excitation of rovibronic transitions in the NO γ ($X\,^2\Pi$, $v''=0 \rightarrow A\,^2\Sigma^+$, $v'=0$) band. Unexpectedly large Stark broadening was observed in the spectrum, even at moderate laser intensities. Therefore, we have studied the Stark effect in some detail to understand the nature of the broadening mechanism.

The experimental arrangement used was described previously in Ref. 5. Selected regions of the $\gamma(0,0)$, two-photon, fluorescence-excitation spectrum were scanned with a dye laser, which was pumped by the third harmonic of a Nd-doped yttrium aluminum garnet laser operated at 10 Hz. A linearly polarized beam was generated at wavelengths near 450 nm, with a 5-nsec pulse duration, an average linewidth of ≈ 0.2 to 0.3 cm^{-1}, and with energies of a few millijoules. The beam intensity distribution was spatially and temporally nonuniform, and varied from pulse to pulse. A large fraction of the beam energy was focused into a sample cell for the Stark measurements. Approximately 10% was split off and loosely focused into a reference cell to provide a simultaneous spectrum with negligible Stark broadening. NO pressures were identical in both cells and ranged from 0.05 to 0.1 Torr, where collisional broadening was negligible.

An example of the broadening for a spectral region in which the line separations are significantly greater than the laser bandwidth is shown in Fig. 1. The upper trace was taken with an average laser intensity of ≈ 3 GW/cm^2. The lower trace, recorded simultaneously with a reduced laser power level, shows a spectrum where the Stark effect is negligible. The upper spectrum displays an asymmetric shift to the blue for both the $S_{11}+R_{21}(20\frac{1}{2})$ and $S_{21}(16\frac{1}{2})$ transitions. The ro-

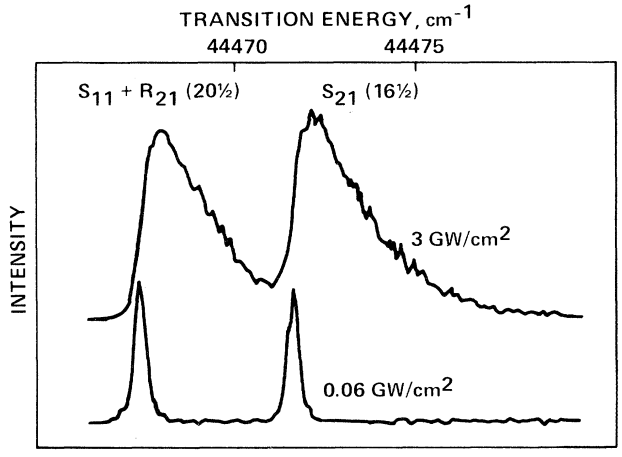

FIG. 1. Experimental two-photon spectra of NO: $X\,^2\Pi$, $v''=0 \rightarrow A\,^2\Sigma^+$, $v'=0$, $S_{11}+R_{21}(20\frac{1}{2})$, and $S_{21}(16\frac{1}{2})$ transitions at low and high laser intensities. NO pressure was 0.1 Torr.

tational sublevels, which are split by the laser field, are not resolved. The splitting appears in the spectrum as a broadening, 3 to 4 cm^{-1} wide. Additionally, the relative heights of the two peaks are reversed. Figure 2 shows a plot of the full width at half maximum (FWHM) of the $S_{11}+R_{21}(20\frac{1}{2})$ and $S_{11}+R_{21}(7\frac{1}{2})$ lines, as a function of the average laser energy. The width is linearly proportional to the pulse energy, indicating a quadratic Stark effect. The intercept at zero energy corresponds to the convoluted two-photon laser width and Doppler width.

To account for the observed Stark effect quantitatively, both shifts and widths induced by the optical field need to be considered. A survey of spectroscopic data[6-8] for NO shows that at the laser frequencies for the two-photon $X \rightarrow A$ transition, each rotational level of the A state is nearly resonant with a one-photon transition to a J level of a high-lying discrete electronic state. The observed splitting can be attributed to near-resonant, one-photon coupling via the Stark field (i.e., a quadratic Stark effect). In addition to the splitting, a significant width is also introduced since the A state can be coupled with the ionization continuum by two-photon transitions, which are enhanced by the near-resonant one-photon step. This additional width corresponds to a quartic Stark effect.

An important factor in determining the magnitude of the observed Stark effect is the resonance-energy gap, G (the difference between the energies of the perturbing state and the sum of the A-state and one-photon energies). From available experimental data,[6-9] the strongest perturbing level of the $S_{11}+R_{21}(20\frac{1}{2})$ branch has been identified as $B\,^2\Pi$, $v=25$; and for the $S_{21}(16\frac{1}{2})$ branch, $K\,^2\Pi$, $v=1$. Also, for the A-state rotational levels considered, the smallest energy gaps vary between 3 and 4 cm^{-1}.

We have calculated the Stark shifts by solving the time-dependent Schrödinger equation directly. The commonly used perturbation approach[2,3] was found to be inadequate, as a result of the small resonance-

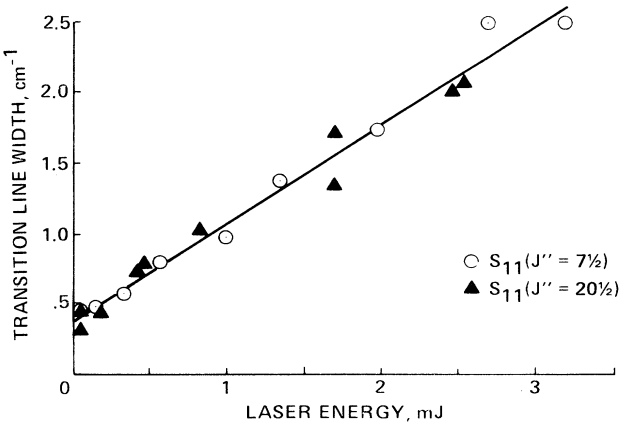

FIG. 2. Linewidth (FWHM) of the $S_{11}+R_{21}(20\frac{1}{2})$ and $S_{11}+R_{21}(7\frac{1}{2})$ lines as a function of laser energy. Focused beam diameter was $\approx 300\ \mu m$. NO pressure was 0.05 Torr.

energy gaps. Calculations were performed for the combined molecule and field system with each rotational level of the A state coupled to six rotational levels of the $B\,^2\Pi$ or $K\,^2\Pi$ state, via dipole interactions; i.e., $J=J_A+1$, J_A, J_A-1 for each of the spin components, F_1 an F_2, of the perturbing state. Contributions from the $X\,^2\Pi$ state were negligible. In the dressed-molecule representation,[10] we can cast the Schrödinger equation into the form of a secular equation.[11] For a state A, coupled to a set of bound states I and J, through the potential V, we have

$$\mathbf{G}+\mathbf{V}-\boldsymbol{\alpha}=0, \tag{1}$$

where $G_{AA}=0$, $G_{IJ}=(E_I-E_A-\omega)\delta_{IJ}$, $V_{AA}=0$, and

$$V_{AI}=-\tfrac{1}{2}\mathscr{E}\,\mu_{AI}\mathscr{R}(J_A,J_I,S_A,S_I,M). \tag{2}$$

Also, $V_{IJ}=0$, because these terms are nonresonant. In Eq. (2), μ_{AI} is the transition dipole moment, $\mathscr{R}$ is a rotational line-shift factor, and $\mathscr{E}$ is the field strength. Associated with each eigenvalue, α_N, there is a

TABLE I. Stark shifts (cm^{-1}) and widths (cm^{-1}) calculated for three rotational levels of the $A\,^2\Sigma^+$, $v=0$ state at $I_{AV}=3$ GW/cm^2.

	$F_1, J=22\frac{1}{2}$		$F_2, J=21\frac{1}{2}$		$F_2, J=18\frac{1}{2}$	
M	Shift	Width	Shift	Width	Shift	Width
$\frac{1}{2}$	−0.03	0.06	−0.41	0.39	−0.02	0.04
$5\frac{1}{2}$	0.99	0.42	−0.25	0.35	1.02	0.70
$10\frac{1}{2}$	2.44	0.52	0.22	0.27	2.41	0.91
$15\frac{1}{2}$	3.83	0.49	1.11	0.21	3.87	0.93
$20\frac{1}{2}$	5.03	0.46	2.53	0.20	· · ·	· · ·

dressed-state wave function,

$$\Psi_N(\mathbf{r},t) = [B_{NA}(\Phi_A,n) + \textstyle\sum_I B_{NI}(\Phi_I,n-1)]\exp\{-i[E_A + (n+\frac{1}{2})\omega - \alpha_N]t\}, \quad (3)$$

where Φ_A and Φ_I are the time-independent molecular eigenfunctions; B_{NA} and B_{NI} are time-independent coefficients; and n is a photon occupation number. The nonstationary wave function, $\Psi(\mathbf{r},t)$, is a linear combination of the Ψ_N's. For the case of two-state coupling,[12] our result agrees with that obtained previously in closed form.[13]

While $\Psi(\mathbf{r},t)$ is oscillatory, the laser probes only one of its components. Since a single laser field was used in this experiment, the probe and Stark frequencies are identical, and are always tuned to the component of $\Psi(\mathbf{r},t)$ with α closest to zero. We designate it as Ψ_0. The eigenvalue, α_0, then corresponds to the Stark shift observed. To determine α_0, Eq. (1) is solved separately for each M rotational sublevel. Since the experiment requires the Stark and probe frequencies to be equal, an iterative solution is required.

The rotational line-shift factor, $\mathscr{R}$, is given by

$$\mathscr{R}(J_A,J_I,S_A,S_I,M) = \left(\frac{2J_A+1}{2J_I+1}\right)^{1/2} C(J_A 1 J_I, M0M) \times \left[\sum_{\Omega_A=-1/2}^{1/2}\sum_{\Omega_I=1/2}^{3/2} \langle A\,^2\Sigma^+,\ J_A \pm \tfrac{1}{2}|A\,^2\Sigma^+,\ \Omega_A\rangle \times C(J_A 1 J_I, \Omega_A 1 \Omega_I)\langle {}^2\Pi,\ J_I \pm \tfrac{1}{2}|{}^2\Pi, \Omega_I\rangle\right]. \quad (4)$$

Here we have assumed the use of a single, linearly polarized laser and intermediate coupling between Hund's cases (a) and (b).

The two-photon rotational line strength, $\mathscr{S}(J_X,J_A,S_X,S_A,M)$, between individual M levels of the $X\,^2\Pi$ and $A\,^2\Sigma^+$ states, determines the shape of the Stark spectrum. The M-dependent line strength can be deduced from the unresolved two-photon rotational line strength of Halpern, Zacharias, and Wallenstein[14] and is given by

$$\mathscr{S}(J_X,J_A,S_X,S_A,M) = \frac{5|C(J_A 2 J_X, M0M)|^2}{2J_X+1}\mathscr{S}(J_X,J_A,S_X,S_A). \quad (5)$$

The Stark width for individual M levels, arising from the interaction of the wave function Ψ_0 with the ionization continuum, is expressed by

$$\Delta\Gamma = \tfrac{1}{2}\pi \textstyle\sum_\lambda |\langle\Phi_{c,\lambda}|\boldsymbol{\mu}\cdot\mathscr{E}|\Psi_0\rangle|^2. \quad (6)$$

The continuum states $\Phi_{c,\lambda}$ are evaluated at energy $E_C = E_A + 2\omega$, and the subscript λ runs over all degenerate quantum numbers. The M dependence of the widths is implicitly contained in rotational factors similar to $\mathscr{R}$. The energy shift, due to coupling to the continuum, was found to be negligibly small.

The vibronic transition moments, μ_{AI}, were calculated from *ab initio* wave functions, using a large (32 σ, 22 π, 6 δ, 4 ϕ) Slater-type basis set containing Rydberg functions.[11] Complete-active-space self-consistent-field calculations were carried out for the $A\,^2\Sigma^+$ state, followed by multireference, first-order, configuration-interaction calculations for both $^2\Sigma$ and $^2\Pi$ symmetries. Transition moments between the B and K states and the ionization continuum were calculated from discretized configuration-interaction wave functions using the Stieltjes imaging method.

The Stark shifts and widths of the three rotational levels of the $A\,^2\Sigma^+$ state under consideration have been calculated for the experimental field intensity, I_{AV}, of 3 GW/cm^2, using a chaotic-field model for the photon statistical behavior.[15] Their values are shown in Table I for representative M levels. Both the shifts and widths are strongly M dependent, as a result of a dominant M^2-dependent term in the rotational line-shift factor. A synthetic, Stark-broadened, two-photon spectrum of NO has been generated with use of the calculated parameters and is presented in Fig. 3. At a given probe frequency in the synthetic spectrum, all transitions that contributed to the intensity were convoluted with the laser and Doppler widths, with use of a Voigt function. The laser width was assumed to be composed of both probe and Stark fields, with an effective, single, Gaussian width of 0.5 cm^{-1}. The vertical lines in Fig. 3 represent the calculated positions of the Stark-shifted M-level transitions at I_{AV}. The experimental spectrum taken at the same field strength is also reproduced in the figure. Comparing the two spectra, we find overall agreement. Both spectra show asymmetric shifts to the blue and a peak-height reversal from the weak-field case. The asymmetry is the result of M-dependent blue shifts and the intensity distributions of the shifted lines. The individual Stark widths smooth the line shape. The discrepancies between the experimental and synthetic spectra are probably due to uncertainties in the parameters used in

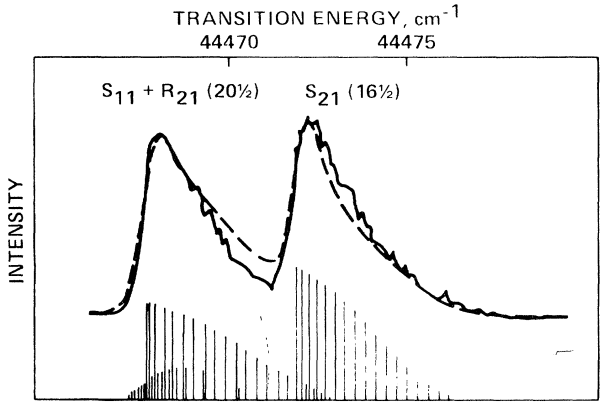

FIG. 3. Comparison of the synthetic (dashed line) and experimental (solid line) high-field spectra (same conditions as Fig. 1). The vertical lines represent the calculated positions of the shifted M levels.

the calculation. The effects of spectral, spatial, and temporal variations in the laser radiation were evaluated with a both time-dependent and spatially variant model, with either Lorentzian or Gaussian spectral distributions. In all reasonable cases, the changes to the synthetic spectral profiles, integrated over all time and space, were less than 10%. Finally, B_J and I_{AV} were varied over a reasonable range of uncertainties with only minor changes observed for the large-M transitions.

In conclusion, a theoretical method has been developed that should be uniquely applicable to near-resonant Stark effects. Several aspects of the model were found to be essential for reproducing the experimental features in NO. In particular, the time-dependent Schrödinger equation had to be solved directly since perturbation methods were unsuccessful. Additionally, an iterative solution of the secular equation was necessary to account for the single-beam experiment properly.

[a]Mailing address: NASA Ames Research Center, Moffett Field, Cal. 94035.

[b]Current affiliation: Polyatomics Research Institute, Mountain View, Cal. 94043.

[1]C. E. Otis and P. M. Johnson, Chem. Phys. Lett. **83**, 73 (1981).

[2]T. Srinivasan, H. Egger, H. Pummer, and C. K. Rhodes, IEEE J. Quantum Electron. **19**, 1270 (1983).

[3]B. Girard, N. Billy, T. Vigue, and J. C. Lehmann, Chem. Phys. Lett. **102**, 168 (1983).

[4]R. L. McKenzie and K. P. Gross, Appl. Opt. **20**, 2153 (1981).

[5]K. P. Gross and R. L. McKenzie, Opt. Lett. **8**, 368 (1983).

[6]E. Miescher and K. P. Huber, in *Spectroscopy,* edited by D. A. Ramsay (Butterworth, Washington, D.C., 1976).

[7]T. Ebata, N. Mikami, and M. Ito, J. Chem. Phys. **78**, 1132 (1983).

[8]T. C. Steimle and H.-T. Liou, Chem. Phys. Lett. **100**, 300 (1983).

[9]R. Gallusser and K. Dressler, J. Chem. Phys. **76**, 4311 (1982).

[10]C. Cohen-Tannoudji and S. Reynaud, J. Phys. B **10**, 345 (1977).

[11]W. M. Huo, K. P. Gross, and R. L. McKenzie, NASA Report No. TM-85964 (unpublished), and unpublished work.

[12]S. H. Autler and C. H. Townes, Phys. Rev. **100**, 703 (1955).

[13]L. D. Landau and E. M. Lifshitz, *Quantum Mechanics* (Pergamon, London, 1958), p. 143.

[14]J. B. Halpern, H. Zacharias, and R. Wallenstein, J. Mol. Spectrosc. **79**, 1 (1980).

[15]P. Zoller and P. Lambropoulos, J. Phys. B **13**, 69 (1980).